Articles

Discovery of Embelin as a Cell-Permeable, Small-Molecular Weight Inhibitor of XIAP through Structure-Based Computational Screening of a Traditional Herbal Medicine Three-Dimensional Structure Database

Zaneta Nikolovska-Coleska,[†] Liang Xu,[†] Zengjian Hu,[†] York Tomita,[‡] Peng Li,[§] Peter P. Roller,[§] Renxiao Wang,[†] Xueliang Fang,[†] Ribo Guo,[†] Manchao Zhang,[†] Marc E. Lippman,[†] Dajun Yang,[†] and Shaomeng Wang*[,†]

University of Michigan Comprehensive Cancer Center, Departments of Internal Medicine and Medicinal Chemistry, University of Michigan, Ann Arbor, Michigan 48109-0934, Lombardi Cancer Center, Georgetown University Medical Center, Washington, DC 20057, and Laboratory of Medicinal Chemistry, National Cancer Institute, FCRDC, Frederick, Maryland 21702-1201

Received August 29, 2003

The X-linked inhibitor of apoptosis (XIAP) is a promising new molecular target for the design of novel anticancer drugs aiming at overcoming apoptosis-resistance of cancer cells to chemotherapeutic agents and radiation therapy. Recent studies demonstrated that the BIR3 domain of XIAP where caspase-9 and Smac proteins bind is an attractive site for designing small-molecule inhibitors of XIAP. Through computational structure-based screening of an in-house traditional herbal medicine three-dimensional structure database of 8221 individual natural products, followed by biochemical testing of selected candidate compounds, we discovered embelin from the Japanese Ardisia herb as a small-molecular weight inhibitor that binds to the XIAP BIR3 domain. We showed that embelin binds to the XIAP BIR3 protein with an affinity similar to that of the natural Smac peptide using a fluorescence polarization-based binding assay. Our NMR analysis further conclusively confirmed that embelin interacts with several crucial residues in the XIAP BIR3 domain with which Smac and caspsase-9 bind. Embelin inhibits cell growth, induces apoptosis, and activates caspase-9 in prostate cancer cells with high levels of XIAP, but has a minimal effect on normal prostate epithelial and fibroblast cells with low levels of XIAP. In stably XIAP-transfected Jurkat cells, embelin effectively overcomes the protective effect of XIAP to apoptosis and enhances the etoposide-induced apoptosis and has a minimal effect in Jurkat cells transfected with vector control. Taken together, our results showed that embelin is a fairly potent, nonpeptidic, cell-permeable, small-molecule inhibitor of XIAP and represents a promising lead compound for designing an entirely new class of anticancer agents that target the BIR3 domain of XIAP.

Introduction

Apoptosis, or programmed cell death, is an essential cell suicide process that is important for normal development, host defense, and suppression of oncogenesis.[1−4] Inappropriate control of apoptosis plays a role in many human diseases, including cancer, autoimmune diseases, and neurodegenerative disorders.[5−7] Defects in the normal apoptosis machinery has been implicated in the resistance of cancer cells to a wide variety of current anticancer drugs.[8] Therefore, key apoptosis regulators are attractive new molecular targets for designing entirely new classes of anticancer drugs aiming at overcoming apoptosis-resistance in cancer cells.[9,10]

The inhibitor of apoptosis proteins (IAPs) were recently discovered as an important class of intrinsic cellular inhibitors of apoptosis,[11−17] although their functions may not be limited to the regulation of apoptosis.[17] XIAP (X-linked IAP) is the most potent inhibitor of apoptosis among all the IAP proteins.[17] XIAP protein potently inhibits both intrinsic and extrinsic apoptosis pathways[17,18] by binding and inhibiting the initiator caspase-9 and effector caspases (caspase-3 and -7),[19−23] whose activity is crucial for the execution of apoptosis. While the third BIR domain (BIR3) selectively inhibits caspase-9, the linker region between BIR1 and BIR2 inhibits caspase-3 and -7. [17,24,25]

Although the precise role of the endogenous XIAP in the pathological process remains far from completely understood, recent data point to an important role of XIAP in the oncogenic process.[25] XIAP protein was found to be widely expressed in human cancer cell lines[26−33] and human cancer tissues.[26] Apoptotic resistance was found to correlate with the expression levels of XIAP in human prostate and non small cell lung cancer cells.[30,34] The direct role of XIAP in the resistance of cancer cells to radiation was demonstrated using an XIAP antisense approach.[35] XIAP blocks apoptosis

* Corresponding author. Shaomeng Wang, Departments of Internal Medicine and Medicinal Chemistry, University of Michigan Comprehensive Cancer Center, University of Michigan, CCGC/3316, 1500 E. Medical Center Dr., Ann Arbor MI 48109-0934. Tel (734) 615-0362. Fax (734) 647-9647. E-mail: shaomeng@umich.edu.
[†] University of Michigan Comprehensive Cancer Center.
[‡] Lombardi Cancer Center.
[§] National Cancer Institute.

10.1021/jm030420+ CCC: $27.50
Published on Web 04/14/2004

induced by taxol in human prostate LNCaP cancer cells[36] and by Apo2L/TRAIL ligand in the hormone-independent human prostate cancer cell lines.[37] Conversely, down regulation of XIAP has been implicated to play an important role in the synergistic induction of apoptosis by complementation with Apo2/TRAIL and actinomycin D in CL-1, DU-145, and PC-3 prostate cancer cells.[38] Down-regulation of antiapoptotic proteins, including XIAP, was implicated in apoptosis induced by protein kinase inhibitors flavopiridol and 7-hydroxy-staurosporine in B-cell chronic lymphocytic leukemia cells.[39] Down-regulation of XIAP protein induces apoptosis in chemoresistant, p53 wild-type human ovarian cancer but not in the p53 mutated or null cells.[40] Inactivation of XIAP has been shown to play a role in apoptosis induced by phenoxodiol in ovarian cancer cells.[41] Down-regulation of XIAP and other IAP proteins was also observed in mitotic arrest and apoptosis induced by epothilone B in cisplatinum- and paclitaxel-resistant ovarian cancer cells.[42] Recently, overexpression of XIAP has been linked to the resistance of human non small cell lung cancer H-460 cells to chemotherapeutic agents.[43] Collectively, these studies demonstrated that XIAP may play a critical role for the resistance of cancer cells to current chemotherapeutic agents, radiation and TRAIL ligand and direct inhibition of XIAP may represent a promising strategy for the development of an entirely new class of anticancer drugs. Because XIAP blocks apoptosis at the downstream effector phase, a point where multiple signaling pathways converge, strategies targeting XIAP may prove to be especially effective to overcome apoptosis resistance of cancer cells.

Several approaches aiming at directly targeting XIAP are currently being explored. Antisense oligonucleotides that were designed to decrease the levels of the mRNA and protein of XIAP have been shown to induce apoptosis and enhance chemotherapeutic activity against human lung cancer cells in vitro and in vivo.[44] Recently, nonpeptidic, small-molecule inhibitors have been identified through high-throughput screening to target the interaction between XIAP and caspase-3.[45] High-throughput assays have recently been established for identification and design of small molecules that bind to the BIR3 domain of XIAP.[47]

We are particularly interested in designing small-molecule inhibitors that target the XIAP BIR3 domain for several reasons. First, the XIAP BIR3 domain potently binds to caspase-9, traps caspase-9 in its inactive monomeric form, and prevents the formation of the active dimer of caspase-9. Although XIAP also directly binds to caspase-3 and −7 through the linker region between its BIR2 and BIR3 domains, its binding to caspase-9 through its BIR3 domain is most important for its antiapoptotic activity. Second, the structural basis of the interaction of the XIAP BIR3 domain with caspase-9 has recently been elucidated in details through the determination of a high-resolution experimental three-dimensional (3D) structure.[49] Third, Smac/DIABLO (second mitochondria-derived activator of caspases, or direct IAP binding protein with low pI), a protein released from mitochondria in response to apoptotic stimuli, was shown to interact directly with the XIAP BIR3 domain and other IAP proteins and promotes apoptosis in cells by antagonizing IAPs and promoting the activity of caspase-9.[50,51] High-resolution 3D structures of Smac protein and peptide in complex with the BIR3 domain of XIAP clearly showed that Smac interacts with the XIAP BIR3 domain through four residues (alanine-valine-proline-isoleucine, or AVPI) at the free N-terminus of Smac and a well-defined binding pocket in XIAP.[52,53] In fact, Smac and caspase-9 share a common four-residue **I**AP **b**inding **m**otif (or IBM) with which to bind to the surface binding groove in the XIAP BIR3 domain.[54,55] In essence, Smac functions as an endogenous inhibitor of XIAP through targeting the XIAP BIR3 domain and removing the inhibitory effect of XIAP to caspase-9 through a competitive binding mechanism. Fourth, in contrast to most other protein−protein interactions, the interaction of the XIAP BIR3 domain with caspase-9/Smac is mediated by a small and well-defined binding groove in the BIR3 domain of XIAP and only four residues in Smac/caspase-9 proteins, making this site especially suitable for designing druglike, small molecule inhibitors of XIAP.[52,53,55] Finally, three independent studies demonstrated that short Smac peptides tethered to a carrier peptide for intracellular delivery overcome resistance of cancer cells to apoptosis and enhance the anticancer activity of current anticancer drugs in vitro and in vivo.[29,48,43] Of significance, these cell-permeable Smac-based peptides have little toxicity to normal cells or tissues in vitro and in vivo.[29,43,48] Importantly, XIAP and cIAP were identified as the primary molecular targets for these Smac-based peptides in cells.[48] It was also shown that the defect in apoptosome activity was restored by cell-permeable Smac peptides by disrupting XIAP-caspase-9 binding in non-small cell lung cancer H460 cells.[43] Thus, these recent studies using cell-permeable Smac-based peptides have provided the important proof-of-concept that targeting the XIAP BIR3 domain represents a promising therapeutic strategy for the design of a new class of anticancer drugs to overcome apoptosis resistance of cancer cells with high levels of XIAP.[29,43,48]

Peptide-based inhibitors derived from Smac and caspase-9 proteins are powerful pharmacological tools to elucidate the antiapoptotic function of XIAP and the role of XIAP in response of cancer cells to chemotherapeutic agents. But peptide-based inhibitors in general have intrinsic limitations as potentially useful therapeutic agents. These limitations include their poor cell-permeability and poor in vivo stability. Indeed, in the published studies,[29,43,48] Smac-based peptide inhibitors had to be fused to carrier peptides to make them relatively cell-permeable. For these reasons, we and other groups are interested in discovering and designing nonpeptidic, small-molecule inhibitors that directly bind to the BIR3 domain of XIAP.[46,47]

Traditional herbal medicine is a rich source for modern, molecular target-specific drug discovery.[56] In the last several decades, a tremendous amount of effort has been invested to isolate individual compounds from traditional herbal medicine and to determine their chemical structures.[57] Many of these natural products have been screened for the anticancer activity in cancer cells and in animal models of human cancer. Although the molecular mechanism of action of a few compounds has been studied, for the majority of these compounds

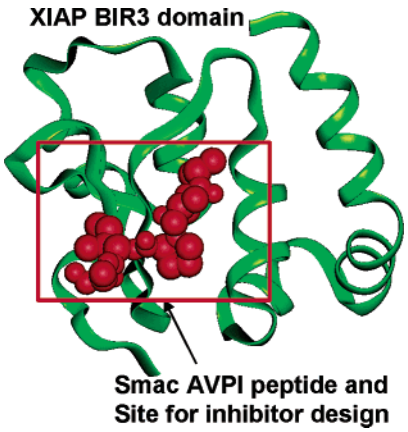

Figure 1. Representation of the experimental 3D structure of the BIR3 domain of XIAP in complex with Smac peptide and the binding site used for computational structure-based database searching of traditional herbal medicine 3D structure database. The XIAP BIR3 is shown in green ribbon, and the Smac peptide is shown in red balls.

isolated from traditional herbal medicine, their precise molecular mechanism of action is not well understood. The lack of the knowledge of the molecular mechanism of these natural products isolated from traditional herbal medicine has impeded their further development as potential useful new anticancer drugs.

Our laboratory is interested in the development of a systematic and structure-based approach to elucidate the underlying molecular mechanism of action of natural products isolated from traditional herbal medicine and importantly to discover promising lead compounds for molecularly targeted anticancer drug discovery. For this purpose, we have built a searchable three-dimensional structure database (TCM-3D) containing 8221 small organic molecules with diverse chemical structures isolated from nearly 1000 traditional Chinese medicinal herbs. Unlike most commercial databases, all the compounds in the TCM 3D-database are natural products derived from traditional medicinal herbs, which have been used for medicinal purposes in China and other countries for centuries. The extensive use of these traditional Chinese medicine recipes in humans has generated a great amount of data about their efficacy and safety. The TCM-3D database is a rich resource for molecularly targeted anticancer drug discovery.

Herein, we wish to report the discovery and characterization of embelin as a fairly potent, nonpeptidic, cell-permeable small molecule inhibitor that targets the XIAP BIR3 domain through computational structure-based computer screening of our in-house TCM-3D.

Results and Discussion

Development and Optimization of an FP-Based Binding Assay. A sensitive, quantitative in vitro fluorescence polarization (FP)-based binding assay was developed in our laboratory based upon the interactions between the XIAP BIR3 domain and Smac protein and peptide.[52,53] Binding of Smac to XIAP is mediated by a few amino acid residues in Smac (Figure 1). In fact, a 4-mer Smac peptide (AVPI)[46] and a 9-mer peptide (AVPIAQKSE)[52] derived from the Smac N-terminus have the same affinities binding to the XIAP BIR3

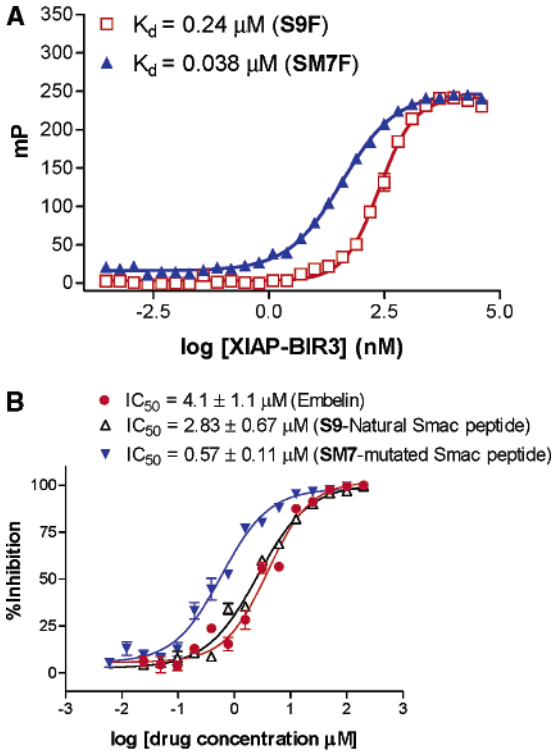

Figure 2. (A) Titration curves of natural Smac peptide (AVPIAQKSEK−FAM, termed **S9F)** mutated Smac peptide (and ARPFAQK−FAM, termed **SM7F**), labeled with 6-carboxyfluorescein succinimidyl ester with XIAP BIR3 protein. (B) Competitive binding curves of the wild-type Smac 9-mer peptide (**S9**), mutated Smac 7-mer peptide (**SM7**), and embelin.

domain as the mature Smac protein. Recently, Kipp et al. has derived a mutated Smac tetrapeptide (ARPF), which has a higher binding-affinity than the natural Smac AVPI peptide.[46] Accordingly, we synthesized two fluorescent labeled Smac peptides: the natural 9-mer Smac (AVPIAQKSEK) and a mutated 7-mer Smac peptide (ARPFAQK) labeled with 6-carboxyfluorescein succinimidyl ester (FAM) as the fluorescence tag (AVPIAQKSEK−FAM, termed **S9F**, and ARPFAQK−FAM, termed **SM7F**, respectively). The unlabeled 9-mer and 7-mer Smac peptides are used as the positive controls. The human XIAP BIR3 protein (residues 241−356) with a His tag is used for this FP-based binding assay.

The dissociation constants (K_d) of the fluorescent labeled **S9F** and **SM7F** peptides to the XIAP BIR3 protein was determined by using a fixed concentration of the peptide (10 nM) and titrating with different concentrations of the protein (0.5 nM to 40 μM). The binding isotherms were produced by a nonlinear least-squares fit to a single-site binding model (Figure 2A). The K_d value for the natural Smac peptide (**S9F)** is 0.24 μM. Consistent with the previous report,[46] **SM7F** showed a higher binding affinity than **S9F**. **SM7F** has an apparent K_d value of 0.038 μM in our FP-based binding assay and is 2 times higher than the K_d value (0.02 μM) measured using a different method.[46] Thus, the obtained K_d values for these two fluorescent labeled Smac peptides using our FP-based assay are similar to the values reported in the literature using other methods.[46,52]

Because the fluorescent labeled mutated Smac peptide (**SM7F**) has a higher binding affinity than the natural Smac peptide, we used this mutated Smac

peptide in our competitive binding assay. We chose to use 10 nM of **SM7F** and 0.060 μM of XIAP BIR3 protein as the assay conditions based on several criteria: 0.060 μM concentration of XIAP is 1.5 times of the K_d value of **SM7F**; 10 nM concentration of **SM7F** is sufficient low to allow the peptide tracer to be more than 50% saturated by 60 nM of the XIAP BIR3 protein and has sufficient fluorescence intensity to overcome the fluorescence background for some inhibitors; under these conditions, the peptide tracer is saturated at over 50% by the XIAP BIR3 protein, which makes the assay very sensitive; and the assay mP range (mP of bound peptide − mP of free peptide) is 95.2 ± 3.0, which gives a large polarization signal window for sensitive detection of the binding of small molecule inhibitors to XIAP in competitive binding experiments.

The specificity of this assay was verified in competition experiments with corresponding unlabeled mutated Smac 7 (**SM**7) and the natural Smac 9-mer (**S9**) peptides. In both cases, the unlabeled peptides were able to abrogate binding of the labeled tracer (Figure 2B). We obtained an IC_{50} value of 2.83 ± 0.67 μM for **S9** and 0.57 ± 0.11 μM for **SM7** (Figure 2B) from three independent experiments in triplicates. The obtained IC_{50} values for these unlabeled Smac peptides are higher than the K_d values of the corresponding fluorescently labeled peptides, but the relative affinities of the two Smac peptides for the XIAP protein correlates well with the published results[46] and their K_d values. The ratio of the K_d values between labeled **SM7F** and **S9F** (7.3 times) and the ratio of the IC_{50} values for the unlabeled **SM7** and **S9** (5.0 times) are similar. The obtained IC_{50} values could be lowered if lower protein concentrations are used, but using too low protein concentrations decreases the signal-to-noise ratio and makes the assay less robust. For this reason, for small molecule inhibitors, their IC_{50} values are reported with the IC_{50} value of the natural Smac peptide (**S9**) and the mutated Smac peptide (**SM7**) under the same conditions for comparison, together with the K_d values of labeled **SM7F** and **S9F**.

Discovery of Embelin as an Inhibitor That Binds to the XIAP BIR3 Domain. Using the DOCK program,[58] we have performed computational structure-based database searching of the TCM-3D database containing 8221 small organic molecules with diverse chemical structures isolated from traditional Chinese medicinal herbs to identify potential small-molecule inhibitors that bind to the XIAP BIR3 domain where caspase-9 and Smac bind. The high-resolution structure of the XIAP BIR3 domain in complex with Smac protein was used to define binding site for the database searching (Figure 1).[52] The sum of the electrostatic and van der Waals interactions as calculated in the DOCK program was used as the ranking score. The top 1000 candidate small-molecules with the best scores were rescored using our recently developed consensus scoring program, X-score.[59] After the reranking, the top 200 compounds were considered as potential small molecule inhibitors of XIAP.

We have obtained samples of 36 potential small-molecule inhibitors primarily from the Developmental Therapeutics Program, the National Cancer Institute, and from commercial sources in some cases and tested

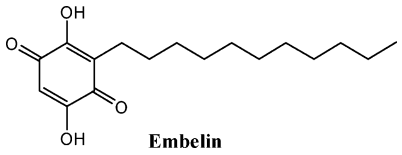

Embelin

Figure 3. Chemical structure of embelin.

their binding affinities to the XIAP BIR3 protein in our optimized FP-based biochemical binding assay as described above. To date, we have discovered five natural products from the TCM-3D that bind to XIAP BIR3 protein and directly compete with **SM7F** peptide. Among these five inhibitors, embelin is the most potent inhibitor, with IC_{50} value of 4.1 ± 1.1 μM (Figure 2B) from three independent experiments in triplicates, which is slightly less potent than the natural 9-mer Smac peptide (IC_{50} value = 2.8 ± 0.7 μM). The chemical structure of embelin is shown in Figure 3.

Conclusive Confirmation of the Binding of Embelin to XIAP BIR3 Where Smac/Caspase-9 Bind by NMR. The FP-based binding assay showed that embelin abrogates the interaction between the Smac peptide and the XIAP BIR3 protein by displacing Smac peptide but does not provide precise direct information on which residues in XIAP embelin binds to. To conclusively confirm that embelin binds to the XIAP BIR3 domain where Smac and caspase-9 bind and rule out any potential false positive, we performed an analysis using nuclear magnetic resonance (NMR) heteronuclear single quantum coherence spectroscopy (HSQC) method. The human XIAP−BIR3 domain (residues 241−356) fused to His-tag was expressed in M9 medium containing ^{15}N ammonium chloride to uniformly label protein with ^{15}N and was purified. ^{15}N HSQC NMR spectra were recorded with embelin and without it at 30 °C. Overlay of two ^{15}N HSQC spectra of the BIR3 domain of human XIAP with embelin (red) and without (black) is shown in Figure 4. Upon the basis of the partially completed backbone assignment, it was found that several residues in XIAP BIR3 protein were affected by the binding of embelin, including W 323 (tryptophan 323) and Y324 (tyrosine 324) residues. Analysis of experimental structures of the XIAP BIR3 domain in complex with Smac protein and peptide and with caspase-9 showed that W323 and Y324 in XIAP are two crucial residues that Smac and caspase-9 interact.[49,52,53] Therefore, our NMR studies conclusively demonstrated that embelin binds to the surface groove in the XIAP BIR3 domain where Smac and caspase-9 bind.

Embelin Selectively Inhibits Cell Growth in Cancer Cells with High Levels of XIAP. We performed a Western blot analysis on the XIAP expression status in several prostate cancer cell lines, as well as in normal prostate epithelial cells (PrEC) and in normal fibroblast WI-38 cells. We found that the widely studied prostate cancer cell lines PC-3, LNCap, CL-1, and DU-145 have high levels of XIAP expression (Figure 5), consistent with previous reports.[26,30] XIAP has a very low level in normal PrEC (Figure 5) and in normal fibroblast WI-38 cells (data not shown).

We evaluated the effect of embelin on cell growth in prostate cancer cells (PC-3 and LNCaP) versus normal cells. Figure 6 shows the representative data of WST-1 cytotoxicity assay which had been repeated for three

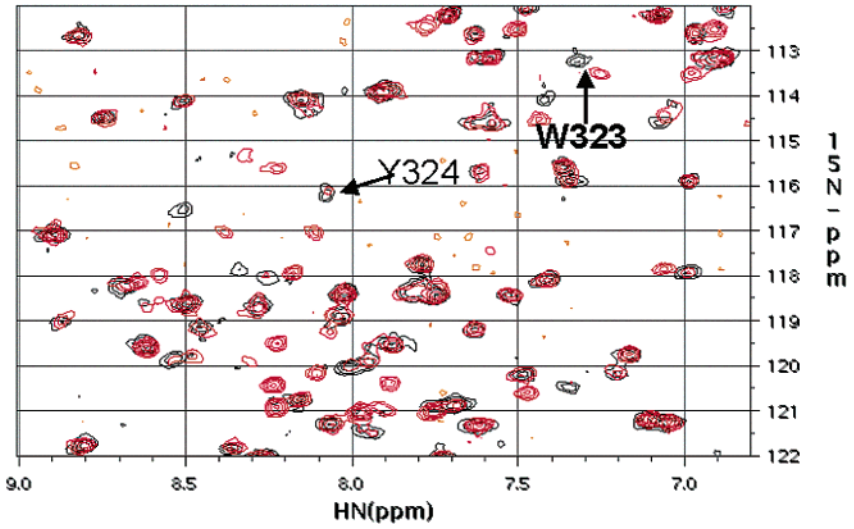

Figure 4. Superposition of ^{15}N-HSQC spectra of free XIAP BIR3 domain (black) and that of the XIAP BIR3 with embelin (red). W323 and Y324 were found to be affected by embelin, similar to Smac, suggesting that embelin and Smac both interact with these common residues

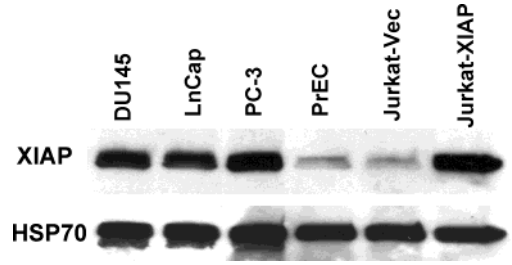

Figure 5. Western blot analysis of the expression of XIAP in human prostate cancer cells and normal cells. 30 μg of cell lysate was loaded per lane on a 12% SDS−PAGE gel, as described in Materials and Methods. The 57 kDa positive band is the expressed XIAP protein. PrEC: normal human prostate epithelial cells. WI-38: normal human fibroblast cell line. HSP70: heat shock protein 70 kDa for gel loading control.

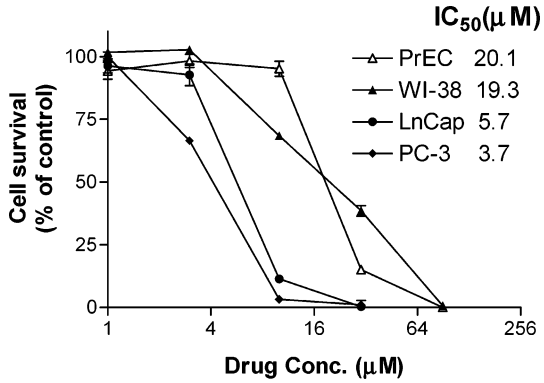

Figure 6. Inhibition of cell growth by embelin in prostate cancer cells (PC-3 and LnCap) and its selectivity in normal human prostate epithelial cells (PrEC) and normal human fibroblast cell line, WI-38. 5000 cells per well in a 96-well cell culture plate were treated with various concentrations of embelin in triplicates. Five days later, the cell growth was measured by WST-1 cell growth assay kit as described in Materials and Methods. The cell growth results are expressed as the % of control and calculated from the % of absorbance of treated wells versus that of vehicle control. IC_{50} value is the drug concentration needed to achieve 50% cell growth inhibition versus control cells.

times with similar results. Embelin inhibited cell growth of both PC-3 and LNCap cells in a dose-dependent manner, with IC_{50} values of 3.7 and 5.7 μM, respectively

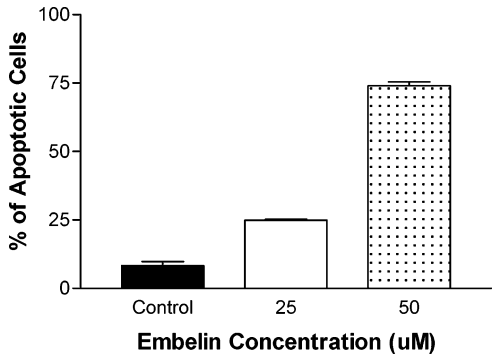

Figure 7. Induction of apoptosis by embelin in PC-3 prostate cancer cells. 1 × 10^6 PC-3 cells per well in six-well culture plates were treated with embelin for 48 h and stained with Annexin V−FITC and propidium iodide for apoptosis by flow cytometry. The results are shown as % of Annexin V−FITC positive apoptotic cells (n = 3).

(Figure 6). To evaluate its selectivity, we also tested its activity in normal PrEC and in WI-38 cells. The IC_{50} values were found to be 20.1 μM and 19.3 μM in normal PrEC and in WI-38 cells, respectively (Figure 6). Thus, embelin appears to display certain selectivity for cancer cells with high levels of XIAP versus normal cells with low levels of XIAP.

Embelin Induces Apoptosis through Activation of Caspase-9 in Cancer Cells with High Levels of XIAP. We further tested embelin for its ability to induce apoptosis in PC-3 prostate cancer cells using the Annexin V−FITC staining. Three separate experiments were performed, which showed that embelin dose-dependently induces apoptosis in PC-3 cells and the results from a representative experiment are shown in Figure 7. After treatment of the cells with 25 and 50 μM of embelin for 48 h, 30% and 75% of PC-3 cells underwent apoptosis, representing approximately 3- and 9-fold increase as compared to control cells, respectively (Figure 7). Of note, higher doses of embelin were used in this apoptosis assay than the WST-1 cytotoxicity assay due to the shorter exposure time (48 h versus 5 days) of embelin to cells.

The most critical antiapoptotic function of XIAP is thought to be mediated by directly binding and inhibit-

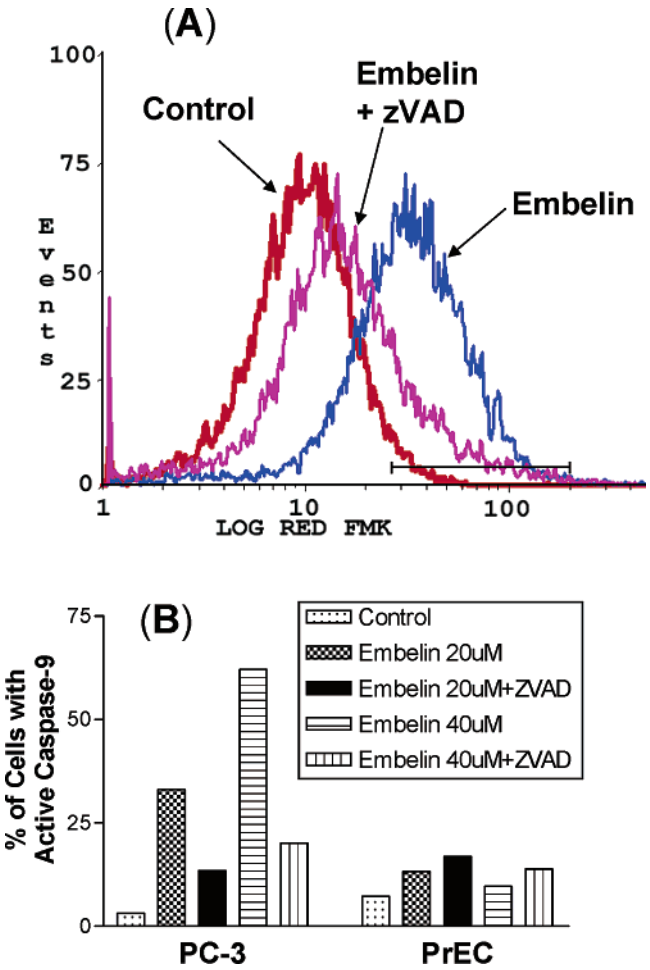

Figure 8. Activation of caspase-9 by embelin in PC-3 prostate cancer cells and its selectivity in normal prostate epithelial cells. (A) Flow cytometry histograms of active caspase-9 stained PC-3 cells that were treated with 40 μM of embelin with or without zVAD, as indicated in the graph. (B) Embelin effectively activates caspase-9 in PC-3 cells in a dose-dependent manner, but has minimal effects on normal PrEC cells. 1 $\times$ 10^6 PC-3 or PrEC cells per well in six-well culture plates were treated with embelin for 42 h. An additional control was prepared by adding the pan-caspase inhibitor Z-VAD-FMK (2 μM final) 5 min before adding embelin, to inhibit caspase activation. The cells were collected and stained for active caspase-9 by CaspGLOW Red Active Caspase-9 Staining Kit and analyzed by flow cytometry in PI channel.

ing caspase-9 via its BIR3 domain, which leads to inhibition of caspase-3.[54] The crystal structure of caspase-9 in complex with the XIAP BIR3 domain shows that the XIAP−BIR3 domain traps caspase-9 in a monomeric state and deprives it of any possibility of catalytic activity.[49] Smac and caspsase-9 compete for the same binding pocket in XIAP BIR3.[49,52,53] Since embelin binds to the BIR3 binding site in XIAP where Smac and caspase-9 bind, we hypothesize that the binding of embelin to XIAP BIR3 will block the binding of XIAP to caspase-9, which subsequently leads to activation of caspase-9. To directly test this hypothesis, we evaluated the ability of embelin to activate caspase-9 in PC-3 cells.

Embelin effectively activates caspase-9 in a dose-dependent manner (Figure 8A and 8B). When treated with 20 and 40 μM of embelin for 42 h, which are the effective doses and optimal time point for embelin to induce early apoptosis, 33.0% and 62.1% of PC-3 cells were positively stained for activated caspase-9, respectively. These represent 10- and 20-fold increase in the activated caspase-9 as compared to vehicle treated control cells (3.1%), respectively. The activation of caspase-9 can be effectively inhibited by zVAD peptide, a pan-caspase inhibitor (Figure 8A and 8B). To evaluate if the activation of caspase-9 by embelin is selective to cancer cells with high levels of XIAP, we also tested embelin in normal PrEC and found that embelin has no significant effect as compared to vehicle treated control cells (Figure 8B). Hence, embelin selectively activates caspase-9 in PC-3 prostate cancer cells with high levels of XIAP and has minimal effect in normal epithelial prostate cells with low levels of XIAP.

To demonstrate that the activation of caspsas-9 and early apoptosis events occurred in the same cells, Annexin V and active caspase-9 double staining was performed on PC-3 cells treated with 40 μM of embelin for 48 h. As shown in Figure 9A-2, PC-3 cells treated with embelin showed intensive active caspase-9 staining in the cytoplasm together with Annexin V−FITC positive staining on the cell membrane, the latter being characteristic of early apoptosis. Figure 9B shows an enlarged view of embelin treated PC-3 cells. Both Annexin V−FITC and active caspase-9 double staining can be blocked by pan-caspase inhibitor zVAD-FMK (Figure 9A-3), indicating that embelin-induced apoptosis requires activation of caspases. In contrast, vehicle control cells show no staining for apoptosis and caspase-9 activation (Figure 9A-1). To rule out nonspecific red fluorescence staining, some of the embelin-treated PC-3 cells were taken out before staining, preincubated with 20 μM of a caspase-9 inhibitor LEHD-FMK for 5 min, then stained for active caspase-9. As shown in Figure 9A-4, preincubation with excessive caspase-9 inhibitor LEHD-FMK blocked the active caspase-9 staining in Annexin V−FITC positive cells (e.g., loss of red signal in Figure 9A-4), but preincubation with excessive caspase-3 inhibitor zDEVD-FMK did not (photo not shown), confirming that the observed red signal was specific for active caspase-9. It is worth noting that virtually only the apoptotic cells show co-staining of both Red (active caspase-9) and Green (Annexin V) fluorescence (Figure 9A-2, 9B-1, and 9B-2), indicating that embelin-induced apoptosis is indeed accomplished by the activation of caspase-9.

Embelin Overcomes the Protective Effect of XIAP to Drug-Induced Apoptosis in XIAP-Transfected Jurkat Cells and Has No Effective in Jurkat Cells Transfected with Vector Control. It has been shown that XIAP overexpression renders the cancer cells resistant to drug-induced apoptosis. We employed stably XIAP-transfected Jurkat cells to investigate whether embelin can attenuate or block the protective effects of XIAP and enhance the chemodrug-induced apoptosis. As shown in Figure 5, Jurkat cells transfected with vector control (Jurkat-Vec) has a very low level of XIAP protein, while Jurkat cells stably transfected with human XIAP has a very high level of XIAP protein.

As shown in Figure 10A, Jurkat cells stably transfected with XIAP (Jurkat-XIAP cells) become resistant to apoptosis induced by etoposide as compared to Jurkat cells transfected with vector control (Jurkat-Vec cells), indicating that XIAP-overexpression protects Jurkat cells from etoposide-induced apoptosis. Consistent with

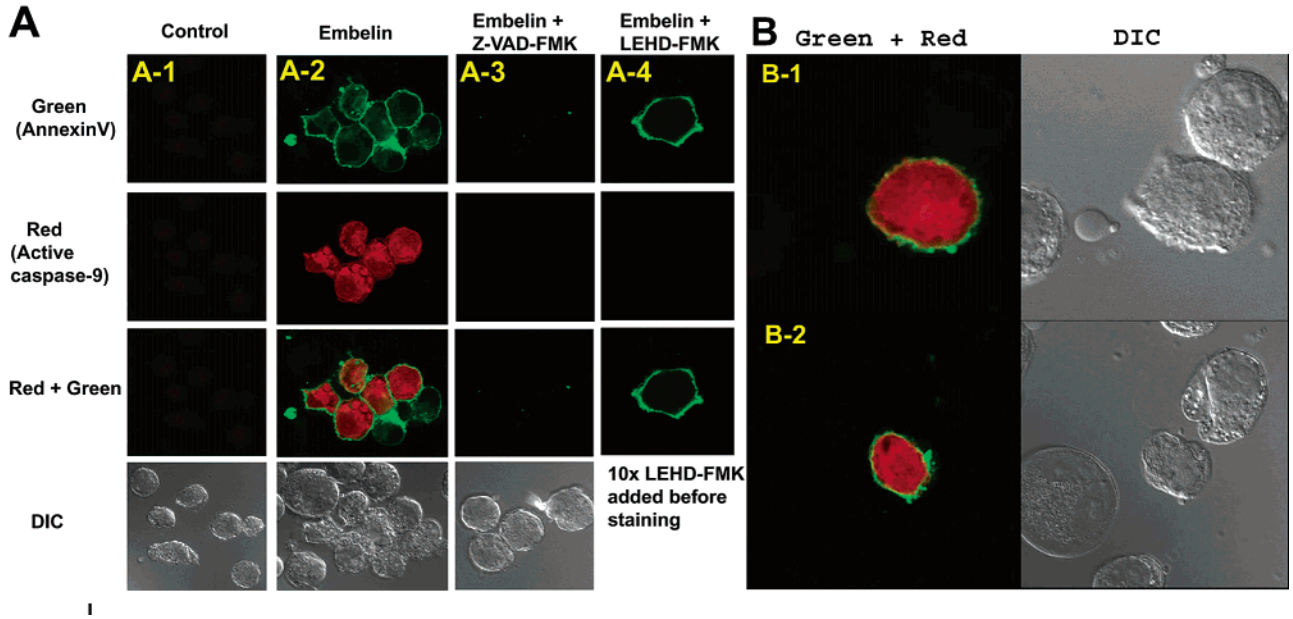

Figure 9. Embelin-induced apoptosis is accompanied by the activation of caspase-9. PC-3 cells were treated with embelin for 48 h and double-stained with Annexin V−FITC and Red Active Caspase-9 Staining Kit, as described in detail in Materials and Methods. A-1: vehicle control; A-2: 40 μM embelin treated; A-3: pan-caspase inhibitor Z-VAD-FMK (1 μM final) was added 5 min before embelin, to inhibit caspase activation; A-4: 40 μM embelin treated as A-2, but preincubated with 20 μM caspase-9 inhibitor LEHD-FMK for 5 min and then stained for active caspase-9. Preincubation with excessive caspase-9 inhibitor blocked the active caspase-9 staining in Annexin V−FITC positive cells and confirmed that the observed red signal was indeed specific active caspase-9. B-1 and B-2: enlarged view of cells from A-2; note that only apoptotic cells show costaining of both red (active caspase-9) and green (Annexin V) fluorescence, indicating that embelin-induced apoptosis is accompanied by the activation of caspase-9. DIC: differential interaction contrast images.

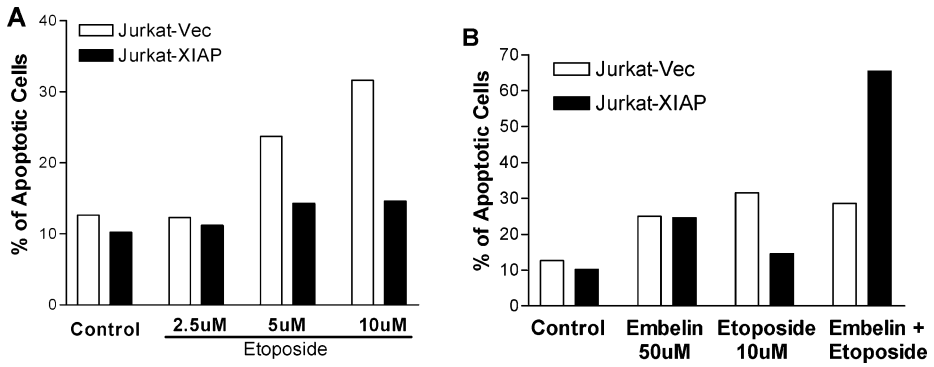

Figure 10. (A) Dose-dependent induction of apoptosis by etoposide in Jurkat cells transfected with vector control (Jurkat-Vec) and stably transfected with XIAP (Jurkat-XIAP cells). (B) Induction of apoptosis by etoposide and embelin alone and in combination in Jurkat-Vec and Jurkat-XIAP cells. 1×10^6 Jurkat-XIAP or Jurkat-Vec cells per well in six-well culture plates were treated with etoposide and embelin alone, or in combination for 15 h, and then stained with Annexin V−FITC and propidium iodide for apoptosis by flow cytometry. The results are shown as % of Annexin V−FITC positive apoptotic cells.

the apoptosis assay, Jurkat-XIAP cells also become less sensitive to etoposide in cell growth assay than Jurkat-Vec cells. While 94.3% ± 0.6% of Jurkat-Vec cells were killed with 2.5 μM of etoposide for 72 h, only 59% ± 2% Jurkat-XIAP cells were killed under the same conditions. Increasing the concentration of etoposide to 10 μM only killed 85% ± 0.1% Jurkat-XIAP cells. These results demonstrated that XIAP overexpression protects the transfected Jurkat cells from etoposide-induced apoptosis and cytotoxicity.

We also evaluated the response of Jurkat-Vec and Jurkat-XIAP cells to embelin in cell growth assays (Figure 11). As expected, embelin only has a weak activity in Jurkat-Vec cells (IC_{50} = 20 μM). Interestingly, embelin also has a weak activity in Jurkat-XIAP cells, essentially identical to that in Jurkat-Vec cells. Of note, both Jurkat-Vec and Jurkat-XIAP cells unlikely depend on the protective effect of XIAP for survival since the parental Jurkat cells have a very low level of XIAP protein. Therefore, treatment of Jurkat-Vec and Jurkat-XIAP cells which do not rely on XIAP protein for survival with a small-molecule inhibitor of XIAP such as embelin is not expected to effectively achieve cell growth inhibition or induce apoptosis.

When used in combination, embelin did not increase etoposide-induced apoptosis as compared to etoposide alone in Jurkat-Vec cells (Figure 10B). This suggests that in cells with a very low level of XIAP protein, XIAP protein plays a minimal role to protect cells from etoposide-induced apoptosis and consequently inhibition of XIAP using a small-molecule inhibitor of XIAP (embelin) has little impact on how cells respond to etoposide. In contrast, combination of embelin and etoposide significantly increases the percentage of apo-

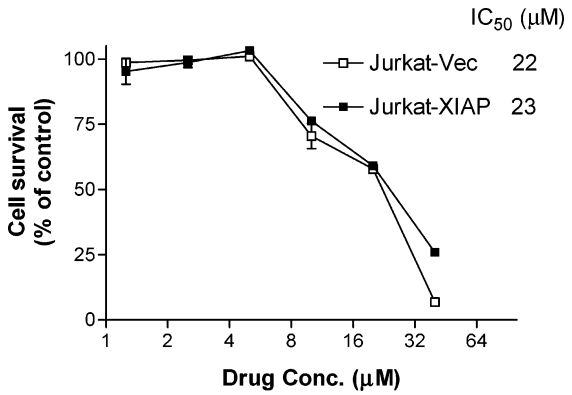

Figure 11. Inhibition of cell growth by embelin in Jurkat cells transfected with empty vector control (Jurkat-Vec) or with XIAP (Jurkat-XIAP) using same assay conditions as described in Figure 6.

ptotic cells as compared to either drug alone in Jurkat-XIAP cells and the effect appears to be more than additive (Figure 10B). This result suggests that when XIAP protein plays a significant role to protect cells from etoposide-induced apoptosis, inhibition of XIAP using a small-molecule inhibitor of XIAP (embelin) overcomes the protective effect of XIAP protein to cells and restores sensitivity of cells to etoposide.

Traditional Herbal Medicine is a Rich Resource for Molecular-Targeted Drug Discovery. Embelin is a plant-based benzoquinone natural product originally isolated from the Japanese Ardisia Herb (*Herba Ardisiae Japonicae*). The Japanese Ardisia Herb has been used as a key ingredient in several traditional Chinese anticancer herbal recipes for the treatment of pancreatic and other types of cancer. Embelin was shown to exhibit significant antitumor activity in methylcholanthrene-induced fibrosarcoma in albino rats,[60] although its cellular molecular mechanism for its anticancer activity was not understood. Our discovery that embelin is a fairly potent inhibitor of XIAP suggests that its anticancer activity is mediated at least in part by its direct binding to XIAP and inhibition of the antiapoptotic function of XIAP protein in cancer cells. Therefore, embelin may represent a promising lead compound that directly targets the BIR3 domain of XIAP for further optimization and development.

Summary

Employing a computational structure-based database searching strategy, we discovered embelin as a potent, nonpeptidic, cell-permeable small molecular-weight inhibitor of XIAP from our in-house traditional herbal medicine 3D structure database containing over 8000 natural products isolated from 885 traditional herbs. Embelin competes with the Smac peptide for binding to XIAP BIR3 protein and has a binding affinity similar to the natural Smac peptide. Using NMR HSQC experiments, we conclusively confirmed that embelin interacts with several key residues in the XIAP BIR3 domain where Smac and caspase-9 bind. Embelin selectively inhibits cell growth in cancer cells with high levels of XIAP protein and has a much less activity in normal cells with low levels of XIAP proteins. Consistent with the proposed underlying molecular mechanism that embelin functions as an inhibitor of XIAP, embelin induces apoptosis in PC-3 prostate cancer cells, which is accompanied by the activation of caspase-9.

Embelin effectively overcomes the protective effects of XIAP to etoposide-induced apoptosis in Jurkat cells stably transfected with XIAP but has no interaction with etoposide in induction of apoptosis in Jurkat cells transfected with vector control, suggesting that embelin directly targets XIAP in Jurkat cells transfected with XIAP and inhibits the ability of XIAP to block apoptosis induced by etoposide. Taken together, our data indicates that embelin represents a promising initial lead compound for the design of an entirely class of anticancer drugs that target XIAP BIR3 domain.

Our present study also demonstrates that traditional herbal medicine is a valuable resource for current molecular-targeted anticancer drug discovery. Our systematic and computational structure-based database searching strategy appears to be effective to discover novel and promising lead compounds for specific molecular targets of interest, and this strategy also helps the elucidation of the possible underlying molecular mechanism of potentially promising anticancer compounds isolated from traditional herbal medicine.

Experimental Section

Traditional Chinese Medicine (TCM) Three-Dimensional Database. We have built a searchable three-dimensional structure database (the TCM 3D-database), which now contains 8221 individual small-molecule weight natural products isolated from 885 traditional herbs. The details of this herbal medicine database and its associated database management tools will be described elsewhere in a separate publication.

The two-dimensional chemical structure of each compound was drawn using the ISIS Draw program,[61] which was saved in the MOL format and then converted into three-dimensional (3D) structures using the Sybyl modeling package.[62] Each 3D structure was minimized using the Sybyl program to obtain a low energy structure. The minimized structures were converted into the Mol2 format for structure-based database screening using the DOCK program.[58]

Computational Structure-Based Database Searching. The experimental 3D structure of the BIR3 domain of XIAP in complex with Smac[52] (pdb code 1G73 from the protein data bank[63]) was used for structure-based database searching of the TCM 3D-database. The program DOCK (version 4.0.1),[63] was used for 3D-database screening to identify potential small-molecule inhibitors of XIAP that can effectively interact with the XIAP BIR3 binding site.

The interactions between Smac protein and BIR3 domain of XIAP protein in the experimental complex structures define the crucial binding elements between them. Thus, the spheres used in the DOCK program were defined by the coordinates of the N-terminal five residues of Smac in the experimental complex structure.[52] All residues of the XIAP BIR3 protein within 8 Å from these five Smac residues were considered as part of the binding site in the screening. United atom KOLLMAN charges were assigned for atoms in the XIAP binding site using the BIOPOLYMER module in the Sybyl program.[62] The Geisterger method as implemented in Sybyl was used to assign charges to all the compounds in the TCM 3D database.

The conformational flexibility of the compounds in the TCM 3D-database was explicitly explored during the database screening in the DOCK program,[58] and their positions and conformations were optimized using single anchor search and torsion minimization. Fifty configurations per ligand building cycle and 100 maximum anchor orientations were used in the anchor-first docking algorithm. All docked configurations were energy minimized using 10 iterations and 2 minimization cycles. A scaling factor of 0.5 was used for the electrostatic

interaction calculations. The sum of the electrostatic and van der Waals interactions as calculated in the DOCK program was used as the ranking score. In the database search, the small molecules were ranked according to their scores as calculated using the energy score function in the DOCK program. The top 1000 candidate small molecules with the best scores were rescored using the recently developed consensus scoring program, X-score.[59] After the reranking, the top 200 compounds were considered as potential small molecule inhibitors of XIAP. To date, we have obtained samples of 36 compounds for testing in biochemical binding assays to the XIAP BIR3 protein.

Fluorescence Polarization Competitive Binding Assay. Asensitive and quantitative in vitro binding assay using the fluorescence polarization (FP)-based method was developed and used to determine the binding affinity of small molecules to XIAP protein. For this assay, fluorescein-5(6)-carboxamidocaproic acid *N*-succinimidyl ester was coupled to the lysine side chain of the mutated peptide, ARPFAQK, derived from the N terminus of a Smac peptide (SM7F), which has been shown to bind to the surface pocket of the XIAP protein with high affinity.[46] The unlabeled peptides, wild type and mutated Smac peptides, were used as the positive control in the binding assay. The recombinant XIAP BIR3 protein of human XIAP (residues 241−356) fused to His-tag was stable and soluble and was used for the FP based binding assay.

Fluorescence polarization experiments were performed in Dynex 96-well, black, round-bottom plates (Fisher Scientific) using the Ultra plate reader (Tecan U. S. Inc., Research Triangle Park, NC). The dose-dependent binding experiments were carried out with serial dilutions of the active compound in DMSO. A 5 μL sample of the tested compound, and preincubated XIAP BIR3 protein (0.060 μM) and SM7F (0.010 μM) in the assay buffer (100 mM potassium phosphate, pH 7.5; 100 μg/mL bovine gamma globulin; 0.02% sodium azide, purchased from InviTrogen Life Technologies), were added to 96-well plates to produce a final volume of 125 μL. For each assay, the bound peptide control containing XIAP BIR3 protein and SM7F (equivalent to 0% inhibition) and free peptide control containing only free SM7F (equivalent to 100% inhibition) were included. The plates were mixed and incubated at room temperature for 3 h to reach equilibrium. IC_{50}, the inhibitor concentration at which 50% of bound peptide is displaced, was determined from the plot using nonlinear least-squares analysis, and curve fitting was performed using GraphPad Prism software.

NMR Experiments. The recombinant BIR3 domain (residues 241−356) of human XIAP protein fused to His-tag (pET28b, Novagen) was overexpressed from *Escherichia coli* BL21(DE3) cells (Nogaven) in M9 medium containing $^{15}NH_4Cl$ as the sole nitrogen source to produce uniformly ^{15}N-labeled protein.[64,65] Most of the protein was found in the soluble fraction, and it was purified using TALON (Clontech) affinity chromatography, followed by G75 size-exclusion chromatography (Pharmacia).

The NMR experiments were performed on a Varian Inova 500 with pulse field gradient (PFG) HSQC, with the water flip back to maximize the signal intensity and to minimize the destruction from the water signal[66,67] (300 μM XIAP, 50 mM phosphate buffer pH 7.3, 2 mM DTT at 25 °C). ^{15}N HSQC NMR spectra were recorded with samples containing 100 μM of the ^{15}N protein in 50 mM Tris (pH 7.2), 50 μM $Zn(Cl)_2$, 1 mM DTT at 30 °C with 100 μM embelin and without it. Then two spectra were compared to identify the chemical shifts induced by the additions of the inhibitor. The NMR data were processed with the programs pipe and nmrDraw.[68,69]

Cell Lines and Reagents. Human prostate cancer cell lines (PC-3, LNCap, CL-1, DU-145) and normal human fibroblast cell line WI-38 were obtained from the American Type Culture Collection (ATCC) and were grown and maintained in Dulbecco's modified Eagle's medium (DMEM) containing 10% FBS (Life Technology, Inc.). Normal human prostate epithelial cells (PrEC) were obtained from Clonetics (Cambrex Inc., MD) and maintained in the special medium provided by the company. Jurkat T-cells stably transfected with either empty vector (Jurkat-Vec), or XIAP(Jurkat-XIAP) were kindly provided by Dr. Colin Duckett at the University of Michigan and were cultured in RPMI 1640 containing 10% fetal calf serum and 1 μg/mL puromycin. Cell cultures were maintained in a humidified incubator at 37 °C and 5% CO_2.

Western Blot Analysis. To analyze the XIAP protein expression in prostate cancer cell lines, Western blot analysis was employed as described previously. Briefly, the cells were lysed at 4 °C in RIPA buffer (50 mM Tris-HCl, pH 7.4, 1% NP-40, 0.25% sodium deoxycholate, 150 mM NaCl), supplemented with a tablet of Mini protease inhibitor cocktail (Roche). The cell lysates (30 μg) were separated on 12% sodium dodecyl sulfate-polyacrylamide gel (Ready-Gel, Bio-Rad, Hercules, CA). The proteins were blotted onto a Hybond nitrocellulose membrane (Amersham, Arlington Heights, IL) and blocked with 2% nonfat dry milk plus 1% BSA (Sigma) in Tris-buffered saline (TBS)/Tween (0.1% Tween-20 in TBS). The blots were incubated with monoclonal anti-XIAP antibody (Transduction Labs, 1:2000) in 10 mL of the 5% BSA for 1 h at room temperature. The blots were washed three times with TBS/Tween and then incubated with horseradish peroxidase coupled ImmunoPure goat anti-mouse antibody (1:20 000) (Pierce, Rockford, IL) in 5% BSA for 1 h at room temperature, washed three times again, and developed with SuperSignal chemiluminescence reagent (Pierce, Rockford, IL). The blots were reprobed with Heat Shock Protein 70kDa (HSK70) antibody (Santa Cruz) as loading control.

Cell Growth Inhibition Assay. Cell growth was determined by the MTT-based assay using Cell Proliferation Reagent WST-1 (Roche) according to the manufacturer's instruction. The WST-1 assay is a colorimetric assay that measures the reduction of WST-1 by mitochondrial succinate dehydrogenase, which belongs to the respiratory chain of the mitochondria and is active only in viable cells. The WST-1 enters the cells and passes into the mitochondria, where it is reduced to a soluble, colored formazan product. The amount of formazan dye formed directly correlates to the number of metabolically active cells in the culture. Cells (5000 cells/well) were grown in medium with 10% FBS, and various concentrations of drugs were added to the cells in triplicates. Four to five days later, WST-1 was added to each well and incubated for 1−3 h at 37 °C. Absorbance was measured with a plate reader at 450 nm with correction at 650 nm. The results are expressed as the % of absorbance of treated wells versus that of vehicle control. IC_{50}, the drug concentration giving 50% growth inhibition was calculated via sigmoid curve fitting using GraphPad Prism 3.0 (GraphPad, Inc.).

Analysis of Apoptosis. PC-3 cells, 1×10^6 cells per well in six-well culture plates, were treated in triplicates with various concentrations of embelin for 24 or 48 h and then trypsinized and washed with PBS. For Jurkat cells, 1×10^6 Jurkat-XIAP or Jurkat-Vec cells per well in six-well culture plates were treated with etoposide, embelin, or both for 15 h. For flow cytometry apoptosis assay, cells were stained with Annexin V−FITC and propidium iodide using the Annexin-V−FLUOS Kit (Roche) according to the manufacturer's instruction. The fluorescence of Annexin V−FITC and propidium iodide of individual cells were analyzed by FACScan. The results are shown as % of Annexin V−FITC positive apoptotic cells.

Activation of Caspase-9 Assay. 1×10^6 PC-3 cells per well in six-well culture plates were treated with various concentrations of embelin, or the same amount of solvent DMSO as vehicle control, for up to 48 h. An additional control was prepared by adding the pan-caspase inhibitor Z-VAD-FMK (1 μM final) 5 min before adding embelin, to inhibit caspase activation. The cells were collected for staining of active caspase-9 by CaspGLOW Red Active Caspase-9 Staining Kit (BioVision, Inc., Mountain View, CA) according to the manufacturer's instructions, with modification. Briefly, to each tube containing 1×10^6 treated or control cells in 0.3 mL complete culture medium were added 1 μL of Red-LEHD-FMK and incubated for 0.5 h at 37 °C incubator with 5% CO_2. For double

staining with Annexin V−FITC, the cells were spun down and resuspended in 100 μL of binding buffer containing 1X Annexin V−FITC from the Annexin-V−FLUOS Kit (Roche) and incubated at room temperature for 10 min. The cells were then washed two times with Wash Buffer from the Active Caspase-9 Staining Kit. The cells were resuspended in 0.3 mL of binding buffer and analyzed by flow cytometry, using PI channel for active caspase-9 and FITC channel for apoptosis.

The active caspase-9 and Annexin V double stained cells were also observed under Zeiss Laser Scanning Confocal Microscope LSM 510 Meta, using the fluorescent filter sets for rhodamine (Red) and FITC (green) channels. Early apoptotic cells show green fluorescence on cell membrane while caspase-9 positive cells show bright red staining in cytoplasm. Photos were taken at original magnification of 630×. Cellular morphology was observed with differential interference contrast (DIC) using DIC channel.

Acknowledgment. Financial support from the Cap CURE Foundation (now the Prostate Cancer Foundation) and the Susan G. Komen Breast Cancer Foundation are greatly appreciated. The initial chemical sample used in our biochemical and biological evaluations was provided by the Drug Synthesis & Chemistry Branch, Developmental Therapeutics Program, Division of Cancer Treatment and Diagnosis, National Cancer Institute, National Institutes of Health; Jurkat T-cells stably transfected with either empty vector (Jurkat-Vec) or XIAP (Jurkat-XIAP) were kindly provided by Professor Colin Duckett, Departments of Pathology and Internal Medicine, University of Michigan, and their help on this project is highly appreciated. We would like to thank Ms. Jane X. Wu for initial compound screening in the FP-based binding assay. The excellent secretarial assistance from Ms. Karen Kreutzer is appreciated.

References

(1) Kerr, J. F.; Wyllie, A. H.; Currie, A. R. Apoptosis: a basic biological phenomenon with wide-ranging implications in tissue kinetics. *Br. J. Cancer* **1972**, *26*, 239−257.
(2) Steller, H. Mechanisms and genes of cellular suicide. *Science* **1995**, *267*, 1445−1449.
(3) Jacobson, M. D.; Weil, M.; Raff, M. C. Programmed cell death in animal development. *Cell* **1997**, *88*, 347−354.
(4) Hengartner, M. O. Programmed cell death in invertebrates. *Curr. Opin. Genet. Dev.* **1996**, *6*, 34−38.
(5) Thompson, C. B. Apoptosis in the pathogenesis and treatment of disease *Science* **1995**, *267*, 1456−1462.
(6) Green, D. R.; Martin, S. J. The killer and the executioner: how apoptosis controls malignancy. *Curr. Opin. Immunol.* **1995**, *7*, 694−703.
(7) Straus, S. E.; Sneller, M.; Lenardo, M. J.; Puck, J. M.; Strober, W. An inherited disorder of lymphocyte apoptosis: the autoimmune lymphoproliferative syndrome. *Ann. Intern. Med.* **1999**, *130*, 591−601.
(8) Igney, F. H.; Krammer, P. H. Death and anti-death: tumour resistance to apoptosis. *Nat. Rev. Cancer* **2002**, *2*, 277−88.
(9) Los, M.; Burek, C. J.; Stroh, C.; Benedyk, K.; Hug, H.; Mackiewicz, A. Anticancer drugs of tomorrow: apoptotic pathways as targets for drug design. *Drug Discovery Today* **2003**, *8*, 67−77.
(10) Reed, J. C. Apoptosis-based therapies. *Nat. Rev. Drug Discov.* **2002**, *1*, 111−21.
(11) Deveraux, Q. L.; Reed, J. C. IAP family proteins-suppressors of apoptosis *Genes Dev.* **1999**, *13*, 239−252.
(12) LaCasse, E. C.; Baird, S.; Korneluk, R. G.; MacKenzie, A. E. The inhibitors of apoptosis (IAPs) and their emerging role in cancer. *Oncogene* **1998**, *17*, 3247−3259.
(13) Kasof, G. M.; Gomes, B. C. Livin, a novel inhibitor of apoptosis protein family member. *J. Biol. Chem.* **2001**, *276*, 3238−3246.
(14) Ambrosini, G.; Adida, C.; Altieri, D. C. A novel anti-apoptosis gene, survivin, expressed in cancer and lymphoma. *Nat. Med.* **1997**, *3*, 917−921.
(15) Deveraux, Q. L.; Takahashi, R.; Salvesen, G. S.; Reed, J. C. X-linked IAP is a direct inhibitor of cell-death proteases. *Nature* **1997**, *388*, 300−304.
(16) Roy, N.; Deveraux, Q. L.; Takahashi, R.; Salvesen, G. S.; Reed, J. C. The c-IAP-1 and c-IAP-2 proteins are direct inhibitors of specific caspases. *EMBO J.* **1997**, *16*, 6914−6925.
(17) Salvesen, G. S.; Duckett, C. S. IAP proteins: blocking the road to death's door. *Nat. Rev. Mol. Cell. Biol.* **2002**, *3*, 401−10.
(18) Fesik, S. W. Insights into programmed cell death through structural biology. *Cell* **2000**, *103*, 273−282.
(19) Takahashi, R.; Deveraux, Q.; Tamm, I.; Welsh, K.; Assa-Munt, N.; Salvesen, G. S.; Reed, J. C. A single BIR domain of XIAP sufficient for inhibiting caspases. *J. Biol. Chem.* **1998**, *273*, 7787−7790.
(20) Sun, C.; Cai, M.; Gunasekera, A. H.; Meadows, R. P.; Wang, H.; Chen, J.; Zhang, H.; Wu, W.; Xu, N.; Ng, S. C.; Fesik, S. W. NMR structure and mutagenesis of the inhibitor-of-apoptosis protein XIAP. *Nature* **1999**, *401*, 818−822.
(21) Asselin, E.; Mills, G. B.; Tsang, B. K. XIAP regulates Akt activity and caspase-3-dependent cleavage during cisplatin-induced apoptosis in human ovarian epithelial cancer cells. *Cancer Res.* **2001**, *61*, 1862−1868.
(22) Riedl, S. J.; Renatus, M.; Schwarzenbacher, R.; Zhou, Q.; Sun, C.; Fesik, S. W.; Liddington, R. C.; Salvesen, G. S. Structural basis for the inhibition of caspase-3 by XIAP. *Cell* **2001**, *104*, 791−800.
(23) Chai, J.; Shiozaki, E.; Srinivasula, S. M.; Wu, Q.; Datta, P.; Alnemri, E. S.; Shi, Y.; Dataa, P. Structural basis of caspase-7 inhibition by XIAP. *Cell* **2001**, *104*, 769−780.
(24) Deveraux, Q. L.; Leo, E.; Stennicke, H. R.; Welsh, K.; Salvesen, G. S.; Reed, J. C. Cleavage of human inhibitor of apoptosis protein XIAP results in fragments with distinct specificities for caspases. *EMBO J.* **1999**, *18*, 5242−5251.
(25) Huang, Y.; Park, Y. C.; Rich, R. L.; Segal, D.; Myszka, D. G.; Wu, H. Structural basis of caspase inhibition by XIAP: differential roles of the linker versus the BIR domain. *Cell* **2001**, *104*, 781−790.
(26) Holcik M, Gibson H, Korneluk RG. XIAP: apoptotic brake and promising therapeutic target. *Apoptosis* **2001**, *6*, 253−61.
(27) Tamm, I.; Kornblau, S. M.; Segall, H.; Krajewski, S.; Welsh, K.; Kitada, S.; Scudiero, D. A.; Tudor, G.; Qui, Y. H.; Monks, A.; Andreeff, M.; Reed, J. C. Expression and prognostic significance of IAP-family genes in human cancers and myeloid leukemias. *Clin. Cancer Res.* **2000**, *6*, 1796−1803.
(28) Wagenknecht B, Glaser T, Naumann U, Kugler S, Isenmann S, Bahr M, Korneluk R, Liston P, Weller M. Expression and biological activity of X-linked inhibitor of apoptosis (XIAP) in human malignant glioma. *Cell Death Differ.* **1999**, *6*, 370−6.
(29) Fulda, S.; Wick, W.; Weller, M.; Debatin, K.-M. Smac agonists sensitize for Apo2L/TRAIL- or anticancer drug-induced apoptosis and induce regression of malignant glioma *in vivo*. *Nat. Med.* **2002**, *8*, 808−815.
(30) McEleny, K. R.; Watson, R. W.; Coffey, R. N.; O'Neill, A. J.; Fitzpatrick, J. M. Inhibitors of apoptosis proteins in prostate cancer cell lines. *Prostate* **2002**, *51*, 133−40.
(31) Hofmann, H. S.; Simm, A.; Hammer, A.; Silber, R. E.; Bartling, B. Expression of inhibitors of apoptosis (IAP) proteins in non small cell human lung cancer. *J. Cancer Res. Clin. Oncol.* **2002**, *128*, 554−60.
(32) Li. J.; Feng. Q.; Kim, J. M.; Schneiderman, D.; Liston, P.; Li, M.; Vanderhyden, B.; Faught, W.; Fung, M. F.; Senterman, M.; Korneluk, R. G.; Tsang, B. K. Human ovarian cancer and cisplatin resistance: possible role of inhibitor of apoptosis proteins. *Endocrinology* **2001**, *142*, 370−80.
(33) Cheng, J. Q.; Jiang, X.; Fraser, M.; Li, M.; Dan, H. C.; Sun, M.; Tsang, B. K. Role of X-linked inhibitor of apoptosis protein in chemoresistance in ovarian cancer: possible involvement of the phosphoinositide-3 kinase/Akt pathway. *Drug Resist. Update* **2002**, *5*, 131−46.
(34) Tang, D. G.; Li, L.; Chopra, D. P.; Porter, A. T. Extended survivability of prostate cancer cells in the absence of trophic factors: increased proliferation, evasion of apoptosis, and the role of apoptosis proteins. *Cancer Res.* **1998**, *58*, 3466−79.
(35) Holcik, M.; Yeh, C.; Korneluk, R. G.; Chow, T. Translational upregulation of X-linked inhibitor of apoptosis (XIAP) increases resistance to radiation induced cell death. *Oncogene* **2000**, *19*, 4174−4177.
(36) Nomura, T.; Mimata, H.; Takeuchi, Y.; Yamamoto, H.; Miyamoto, E.; Nomura, Y. The X-linked inhibitor of apoptosis protein inhibits taxol-induced apoptosis in LNCaP cells. *Urol Res.* **2003**, *31*, 37−44.
(37) Ng, C. P.; Bonavida, B. X-linked inhibitor of apoptosis (XIAP) blocks Apo2 ligand/tumor necrosis factor-related apoptosis-inducing ligand-mediated apoptosis of prostate cancer cells in the presence of mitochondrial activation: sensitization by overexpression of second mitochondria-derived activator of caspase/direct IAP-binding protein with low pl (Smac/DIABLO). *Mol Cancer Ther.* **2002**, *1*, 1051−8.
(38) Ng, C. P.; Zisman, A.; Bonavida, B. Synergy is achieved by complementation with Apo2L/TRAIL and actinomycin D in Apo2L/TRAIL-mediated apoptosis of prostate cancer cells: role of XIAP in resistance. *Prostate* **2002**, *53*, 286−99.

(39) Kitada, S.; Zapata, J. M.; Andreeff, M.; Reed, J. C. Protein kinase inhibitors flavopiridol and 7-hydroxy-staurosporine down-regulate antiapoptosis proteins in B-cell chronic lymphocytic leukemia. *Blood* **2000**, *96*, 393−7.
(40) Sasaki, H.; Sheng, Y.; Kotsuji, F.; Tsang, B. K. Down-regulation of X-linked inhibitor of apoptosis protein induces apoptosis in chemoresistant human ovarian cancer cells. *Cancer Res.* **2000**, *60*, 5659−66.
(41) Kamsteeg, M.; Rutherford, T.; Sapi, E.; Hanczaruk, B.; Shahabi, S.; Flick, M.; Brown, D.; Mor, G. Phenoxodiol-an isoflavone analog-induces apoptosis in chemoresistant ovarian cancer cells. *Oncogene* **2003**, *22*, 2611−20.
(42) Griffin, D.; Wittmann, S.; Guo, F.; Nimmanapalli, R.; Bali, P.; Wang, H. G.; Bhalla, K. Molecular determinants of epothilone B derivative (BMS 247550) and Apo-2L/TRAIL-induced apoptosis of human ovarian cancer cells. *Gynecol. Oncol.* **2003**, *89*, 37−47.
(43) Yang, L.; Mashima, T.; Sato, S.; Mochizuki, M.; Sakamoto, H.; Yamori, T.; Oh-Hara, T.; Tsuruo, T. Predominant suppression of apoptosome by inhibitor of apoptosis protein in non small cell lung cancer H460 cells: therapeutic effect of a novel polyarginine-conjugated Smac peptide. *Cancer Res.* **2003**, *63*, 831−37.
(44) Hu, Y.; Cherton-Horvat, G.; Dragowska, V.; Baird, S.; Korneluk, R. G.; Durkin, J. P.; Mayer, L. D.; LaCasse, E. C. Antisense oligonucleotides targeting XIAP induce apoptosis and enhance chemotherapeutic activity against human lung cancer cells in vitro and in vivo. *Clin Cancer Res.* **2003**, *9*, 2826−36.
(45) Wu, T. Y.; Wagner, K. W.; Bursulaya, B.; Schultz, P. G.; Deveraux, Q. L. Development and Characterization of Nonpeptidic Small Molecule Inhibitors of the XIAP/Caspase-3 Interaction. *Chem Biol.* **2003**, *10*, 759−67.
(46) Kipp, R. A.; Case, M. A.; Wist, A. D.; Cresson, C. M.; Carrell, M.; Griner, E.; Wiita, A.; Albiniak, P. A.; Chai, J.; Shi, Y.; Semmelhack, M. F.; McLendon, G. L. Molecular targeting of inhibitors of apoptosis proteins based on small molecule mimics of natural binding partners. *Biochemistry* **2002**, *41*, 7344−49.
(47) Glover, C. J.; Hite, K.; DeLosh, R.; Scudiero, D. A.; Fivash, M. J.; Smith, L. R.; Fisher, R. J.; Wu, J. W.; Shi, Y.; Kipp, R. A.; McLendon, G. L.; Sausville, E. A.; Shoemaker, R. H. A high-throughput screen for identification of molecular mimics of Smac/DIABLO utilizing a fluorescence polarization assay. *Anal. Biochem.* **2003**, *320*, 157−69.
(48) Arnt, C. R.; Chiorean, M. V.; Heldebrant, M. P.; Gores, G. J.; Kaufmann, S. H. Synthetic Smac/DIABLO Peptides Enhance the Effects of Chemotherapeutic Agents by Binding XIAP and cIAP1 in Situ. *J. Biol. Chem.* **2002**, *277*, 44236−43.
(49) Shiozaki, E. N.; Chai, J.; Rigotti, D. J.; Riedl, S. J.; Li, P.; Srinivasula, S. M.; Alnemri, E. S.; Fairman, R.; Shi, Y. Mechanism of XIAP-mediated inhibition of caspase-9. *Mol. Cell* **2003**, *11*, 519−27.
(50) Du, C.; Fang, M.; Li, Y.; Li, L.; Wang, X. Smac, a mitochondrial protein that promotes cytochrome *c*-dependent caspase activation by eliminating IAP inhibition. *Cell* **2000**, *102*, 33−42.
(51) Verhagen, A. M.; Ekert, P. G.; Pakusch, M.; Silke, J.; Connolly, L. M.; Reid, G. E.; Moritz, R. L.; Simpson, R. J.; Vaux, D. L. Identification of DIABLO, a mammalian protein that promotes apoptosis by binding to and antagonizing IAP proteins. *Cell* **2000**, *102*, 43−53.
(52) Wu, G.; Chai, J.; Suber, T. L.; Wu, J. W.; Du, C.; Wang, X.; Shi, Y. Structural basis of IAP recognition by Smac/DIABLO. *Nature* **2000**, *408*, 1008−12.
(53) Liu, Z.; Sun, C.; Olejniczak, E. T.; Meadows, R. P.; Betz, S. F.; Oost, T.; Herrmann, J.; Wu, J. C.; Fesik, S. W. Structural basis for binding of Smac/DIABLO to the XIAP BIR3 domain. *Nature* **2000**, *408*, 1004−8.
(54) Srinivasula, S. M.; Hegde, R.; Saleh, A.; Datta, P.; Shiozaki, E.; Chai, J.; Lee, R. A.; Robbins, P. D.; Fernandes-Alnemri, T.; Shi, Y.; Alnemri, E. S. A conserved XIAP-interaction motif in caspase-9 and Smac/DIABLO regulates caspase activity and apoptosis. *Nature* **2001**, *410*, 112−6.
(55) Shi, Y. A conserved tetrapeptide motif: potentiating apoptosis through IAP-binding. *Cell Death Differ.* **2002**, *9*, 93−95.
(56) Engel, L. W.; Straus, S. E. Development of therapeutics: opportunities within complementary and alternative medicine. *Nature Reviews: Drug Discovery* **2002**, *1*, 229-.
(57) Yan, X.; Zhou, J.; Xie, G. *Traditional Chinese Medicines: Molecular Structures, Natural Source, and Applications*; Ashgate Publishing Limited: Brookfield, VT, 1999.
(58) Ewing, T. J.; Makino, S.; Skillman, A. G.; Kuntz, I. D. DOCK 4.0: search strategies for automated molecular docking of flexible molecule databases. *J. Comput. Aided Mol. Des.* **2001**, *15*, 411−28.
(59) Wang, R.; Lai, L.; Wang, S. Further development of consensus scoring functions for structure-based drug design. *J. Comput. Aided Mol. Des.* **2002**, *16*, 11−26.
(60) Chitra, M.; Sukumar, E.; Suja, V.; Devi, C. S. Antitumor, antiinflammatory and analgesic property of Embelin, a plant product. *Chemotherapy* **1994**, *40*, 109−13.
(61) ISIS DRAW is a product of MDL Information Systems, Inc., 14600 Catalina Street, San Leandro, CA 94577.
(62) Sybyl, a molecular modeling system, is supplied by Tripos, Inc., St. Louis, MO 63144.
(63) Berman, H. M.; Westbrook, J.; Feng, Z.; Gilliland, G.; Bhat, T. N.; Weissig, H.; Shindyalov, I. N.; Bourne, P. E. The Protein Data Bank. *Nucleic Acids Res.* **2000**, *28*, 235−242.
(64) Cai, M. L.; Huang, Y.; Sakaguchi, K.; Clore, G. M.; Gronenborn, A. M.; Craigie, R. An efficient and cost-effective isotope labeling protocol for proteins expressed in *Escherichia coli*. *J. Biomol. NMR* **1998**, *11*, 97−102.
(65) Jansson, M.; Li, Y. C.; Jendeberg, L.; Anderson, S.; Montelione, G. T.; Nilsson, B. High-level production of uniformly N-15- and C-13-enriched fusion proteins in *Escherichia coli*. *J. Biomol. NMR* **1996**, *7*, 131−141
(66) Grzesiek, S.; Bax, A. The Importance of Not Saturating H_2O in Protein NMR-Application to Sensitivity Enhancement and Noe Measurements. *J. Am. Chem. Soc.* **1993**, *115*, 12593−94.
(67) Sheppard, G. S.; Davidsen, S. K.; Fesik, S. W.; Steinman, D. H.; Carrera, G. M.; Florjancic, A. S.; Hajduk, P. J.; Shuker, S. B.; Olejniczak, E. T.; Nettesheim, D.; Meadows, R. P.; Nagy, I.; Marcotte, P.; Magoc, T. J.; Morgan, D. W.; Summers, J. B. SAR by NMR as a novel tool for lead generation: Discovery of a potent series of non-peptide inhibitors of stromelysin (MMP-3). *Abstr. Pap.-Am. Chem. Soc.* **1997**, *213*, 81.
(68) Delaglio, F.; Grzesiek, S.; Vuister, G. W.; Zhu, G.; Pfeifer, J.; Bax, A. NMRPipe: a multidimensional spectral processing system based on UNIX pipes. *J. Biomol. NMR* **1995**, *6*, 277−293.
(69) Garrett, D. S.; Powers, R.; Gronenborn, A. M.; Clore, G. M. A common sense approach to peak picking in two-, three-, and four-dimensional double and triple-resonance heteronuclear magnetic resonance spectroscopy. *J. Magn. Reson., Ser. B* **1991**, *95*, 214−220.

JM030420+